Reactions of hydrazine with the amidogen radical and atomic hydrogen

Yide Gao,[a] I.M. Alecu,[a] Hamid Hashemi,[b] Peter Glarborg[b,*] and Paul Marshall[a,*]

[a]*Department of Chemistry and Center for Advanced Scientific Computing and Modeling, University of North Texas, 1155 Union Circle #305070, Denton, Texas 76203, USA*
[b]*Department of Chemical and Biochemical Engineering, Technical University of Denmark, DK-2800 Kgs. Lyngby, Denmark*

Abstract

The rate coefficient k_1 for $NH_2 + N_2H_4$ was measured to be $(5.4 \pm 0.4) \times 10^{-14}$ cm^3 molecule^{-1} s^{-1} at 296 K. NH_2 was generated by pulsed laser photolysis of NH_3 at 193 nm, and monitored as a function of time by pulsed laser-induced fluorescence excited at 570.3 nm under pseudo-first order conditions in the presence of excess N_2H_4 in an Ar bath gas. This reaction was also investigated computationally, with geometries and scaled frequencies obtained with M06-2X/6-311+G(2df,2p) theory, and single-point energies from CCSD(T)-F12b/cc-pVTZ-F12 theory, plus a term to correct approximately for electron correlation through CCSDT(Q). Three connected transition states are involved and rate constants were obtained via Multistructural Improved Canonical Variational Transition State Theory with Small Curvature Tunneling. Combination of experiment and theory leads to a recommended rate coefficient for hydrogen abstraction of $k_1 = 6.3 \times 10^{-23}$ T$^{3.44}$ exp(+289 K/T) cm^3 molecule^{-1} s^{-1}. The minor channel for $H + N_2H_4$ forming $NH_2 + NH_3$ was characterized computationally as well, to yield 5.0×10^{-19} T$^{2.07}$ exp(-4032 K/T) cm^3 molecule^{-1} s^{-1}. These results are compared to several discordant prior estimates, and are employed in an overall mechanism to compare with measurements of half-lives of hydrazine in a shock tube.

Keywords: hydrazine, experiment, ab initio calculations, amine chemistry, kinetic modeling

---

*Corresponding authors.

1. Introduction

There is interest in the possible application of ammonia as a carbon-free energy transfer fuel [1, 2]. Its combustion involves high transient concentrations of amidogen (NH_2) radicals, and thus significant formation of hydrazine (N_2H_4) as a reactive intermediate, via NH_2 recombination. Development of quantitative mechanisms for analysis of practical combustion conditions requires detailed information about the kinetics and product branching ratios for the important chemical steps in the transformation of NH_2 and N_2H_4. Such information is also relevant to the use of hydrazine as a propellant, and in the interpretation of laboratory experiments designed to probe simplified chemical systems such as high-temperature flow-tube, CSTR, shock tube and rapid-compression experiments which characterize species profiles, pyrolysis products and ignition delays for N_2H_4, NH_3 and/or blends with hydrocarbon species that promote faster burning.

Here we focus on two processes. The first is hydrazine's interaction with amidogen radicals

$$NH_2 + N_2H_4 \rightarrow NH_3 + N_2H_3 \qquad (R1)$$

Li and Zhang illustrated a variety of estimated rate coefficients k_1 which span three orders of magnitude near 1000 K [3]. We have plotted some assessments in Fig. 1.

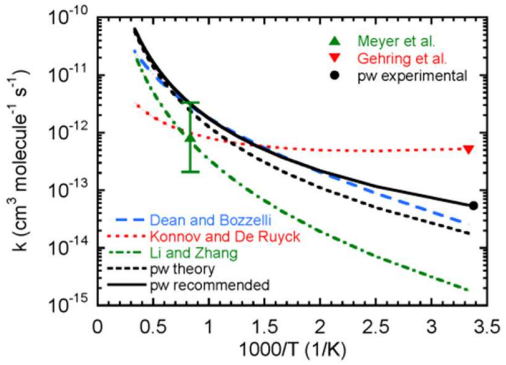

Fig. 1. Arrhenius plot of some evaluations of the rate coefficient for $NH_2 + N_2H_4$. ▲ Meyer et al. [4], ▼ Gehring et al. [5], dotted red line Konnov and De Ruyck [6], green dash-dot line Li and Zhang [3], blue dashed line Dean and Bozzelli [7], dashed black line present quantum calculations, ● present measurement, solid black line present recommendation.

At room temperature, Gehring et al. [5] obtained k_1 and other kinetics by fitting species profiles after mixing flows of hydrazine and H atoms, monitored with ESR and mass spectrometry, and interpreted with a multi-step mechanism. At ca. 1200 K, Meyer et al. [4] analyzed R1 via its influence as part of secondary chemistry following dissociation of N_2H_4 to NH_2 radicals in a shock tube. Konnov and De Ruyck used a rate expression that connects these two determinations in their studies of hydrazine flames [6]. These flames are remarkable for not requiring an oxidizer, and lead exothermically to NH_3, N_2 and H_2. Konnov and De Ruyck highlighted particular sensitivity of the flame speed to the value of k_1 [6]. We also note two theoretical studies. Dean and Bozzelli used an empirical approach to estimate modified Arrhenius parameters [7]. Li and Zhang applied quantum chemistry methods [3]. As can be seen, the difference between the largest and smallest k_1 at room temperature from these approaches is more than a factor of 200. We apply the laser photolysis/laser-induced fluorescence (LP-LIF) technique to obtain the first isolated elementary reaction data for reaction 1, at room temperature, and investigate the temperature dependence of k_1 via quantum chemistry methods.

Hydrogen atoms are typically an abundant radical in combustion. The total rate constant k_2 for N_2H_4 consumption by reaction with H-atoms has been measured under isolated reaction conditions by Vaghjiani (see ref [8] and references therein). There are two plausible channels with ground-state products

$$H + N_2H_4 \rightarrow H_2 + N_2H_3 \qquad (R2a)$$

$$\rightarrow NH_3 + NH_2 \qquad (R2b)$$

and the dominant pathway is thought to be 2a, H-atom abstraction. Theoretical analysis of R2a is in accord with measurements [9, 10]. Here we determine k_{2b} for the minor N-N breaking pathway computationally. Ghosh and Bair studied chemi-luminescence attributed to electronically-excited NH_2 formed via

$$H + N_2H_4 \rightarrow NH_3 + NH_2(A\,^2A_1) \qquad (R2c)$$

and over 293-349 K measured $k_{2c}/k_2 = 3.4 \times 10^{-4}$ exp(-303 K/T) [11]. Konnov and De Ruyck relied on this ratio to derive k_{2b} for modeling hydrazine flames

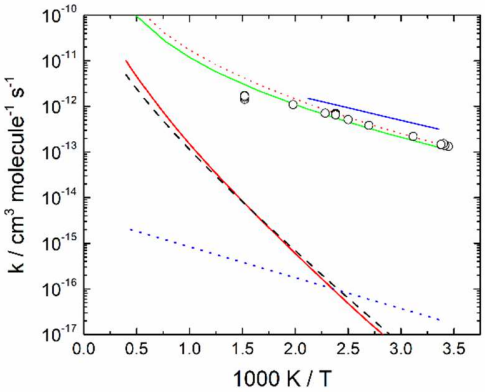

Fig. 2. Arrhenius plot for $H + N_2H_4$ (a) forming $NH_3 + NH_2$ derived from experiments (blue dotted line, Konnov and De Ruyck [6]) and computations (black dashed line, Hwang and Mebel [12]; red line, present work) and (b) forming $H_2 + N_2H_3$ derived from experiments (blue line, Gehring et al. [5]; circles, Vaghjiani [8]) and computations (red dotted line, Li et al. [9]; green line, Kanno and Tito [10]).

[6], which was also used by Alturaifi et al. in their study of ammonia pyrolysis [13].There has been one prior computational determination of k_{2b} by [12].

These two evaluations of k_{2b} are plotted in Fig. 2; the significant differences motivate our renewed attention to this system. Our new results for reactions 1 and 2 are then incorporated into a chemical kinetic model and applied to selected experimental systems to investigate their impact.

2. Methodology

2.1 Experimental

Kinetics of NH_2 radicals were measured by the laser photolysis/LIF technique. Details of the apparatus have been provided elsewhere [14, 15]. The general approach is to generate a pulse of NH_2 in the presence of an excess of N_2H_4 and to monitor the reduction in concentration $[NH_2]$ with time, with microsecond resolution, by exciting LIF at various delays after initiation. 193 nm excimer laser pulses at energy F photolyze NH_3. Low energies are employed to keep the initial concentration $[NH_2]_0$ small to avoid secondary chemistry involving other photofragments or reaction products. The 193 nm beam cross section is ca. 0.6 cm^2. $[NH_2]_0$ is estimated from $[NH_3]$ and its absorption cross section at 193 nm, but is not needed to determine the rate constant k_1 for reaction 1. LIF at wavelengths above 590 nm (selected with a cutoff filter) is excited by dye-laser pulses, with energy E, tuned to the 570.3 nm A $^2A_1 \leftarrow$ X $^2B_1$ transition from the ground electronic state of NH_2. A photomultiplier tube and boxcar integrator average the LIF intensity, proportional to $[NH_2]$, from multiple shots at various fixed delays after the UV initiation pulse. Experiments are carried out in a large excess of Ar bath gas at pressure P (10-30 mbar) which slows diffusion of reactive species to the walls of the reaction cell, so that the monitored chemistry occurs in an effectively wall-less reaction zone defined by the intersection of the photolysis and probe laser beams. The bath gas also thermalizes reactants and products whose temperature T is monitored with a retractable thermocouple, corrected for radiation errors. A slow flow of gas into the reaction cell replenishes reagents in the reaction zone between UV laser pulses (repeated at 5 Hz). The average residence time of gas in the reaction cell before photolysis is τ_{res}.

$[N_2H_4]$ is 2-3 orders of magnitude greater than $[NH_2]_0$, so that $[N_2H_4]$ is effectively constant while NH_2 reacts, and the bimolecular reaction 1 is studied under pseudo-first-order conditions where $d[NH_2]/dt = -k_{ps1}[NH_2]$ with $k_{ps1} = k_1[N_2H_4] + k_{diff}$. k_{diff} accounts for diffusional loss of NH_2 out of the reaction zone, which is observed to be effectively first-order, plus any other losses that do not depend on $[N_2H_4]$. k_{ps1} is found from an exponential decay fit to the LIF vs time. A linear plot of k_{ps1} vs $[N_2H_4]$ has slope k_1.

2.2 Computational

Reaction 1 was analyzed computationally. Geometries and harmonic vibrational frequencies of the reactants, transition states (TSs) and products were derived via density functional theory, with the M06-2X functional and MG3S basis set (equivalent to 6-311+G(2df,2p) here) implemented in the Gaussian program [16]. Comparison of the observed fundamental frequencies vs calculated harmonic values for NH_2, N_2H_4 and NH_3 yields a scale factor of 0.945, applied to all species to obtain fundamental frequencies which are used in the kinetic calculations. We use a factor of 0.97 [17] to derive anharmonic vibrational zero-point energies, used in determination of relative enthalpies at 0 K. Next, single-point energies were obtained at higher levels of theory. The Molpro program [18] was used to obtain CCSD(T)-F12b/cc-pVTZ-F12 energies, which represent an approximate extrapolation of coupled cluster theory with perturbative triple excitations to the complete basis set limit. These results are summarized in Tables S2 and S3.

This is sufficient information for a canonical transition state theory (TST) calculation of the rate constant. To incorporate variational effects, points along the reaction path in the TS region were characterized with a dual-level approach. Geometry and vibrations were derived with M06-2X//6-311+G(2df,2p) theory. The energy of the region was adjusted to match that from more accurate evaluation at the saddle point. Preliminary tests were made with W1U theory [19], but then corrected to approximate CCSDT(Q) complete basis set results (see below). Multi-structural canonical variational TST with optimized multi-dimensional tunneling (MS-CVT/μOMT) developed by Truhlar and coworkers [20, 21] was applied via the Polyrate program [22].

A multi-structural torsion approach is applied because, as noted by Li and Zhang [3], there are three distinct TSs for attack by NH_2 on N_2H_4. They can interconvert via torsions of hindered internal rotors. Each TS has a mirror image, as does hydrazine, while NH_2 and N_2H_4 with C_{2V} and C_2 symmetry, respectively, both have rotational symmetry numbers of 2. We incorporate the impact of multiple TSs, and torsion in N_2H_4, on molecular partition functions via the MSTor code [23] of Truhlar and coworkers. The general description and the details of the exact algorithm we applied may be found elsewhere [24]. The influence of torsions between multiple conformations is expressed in terms of correction factors F to the vibrational partition functions.

Because CCSD(T) is a good but incomplete treatment of electron correlation, we corrected the energy in the TS region by the quantity ΔQ = E(CCSDT(Q))-E(CCSD(T)) evaluated with the cc-pVDZ basis set, for the reactants and saddle point. This further improves the correlation treatment, to the full triples plus perturbative quadruples level.

Improved basis set extrapolation may have an influence, which is addressed empirically (see later). Other factors found to be negligible (see Table 3S) are core-valence, scalar relativistic and diagonal Born-Oppenheimer corrections, with impacts ≤0.3 kJ mol^{-1}) on the barrier. The T1 diagnostic was highest at 0.026 for TS2, within bounds where CCSD theory is valid for open-shell species [25].

Reaction 2 was also investigated computationally. Geometries and frequencies were obtained with M06-2X/6-311+G(2df,2p) theory as before, with the same scale factors to derive anharmonic zero-point energy and fundamental frequencies. Single-point energies were calculated at the CCSD(T)-F12b/cc-pVQZ-F12 level. Canonical TST was applied with the Multiwell program suite [26], with all modes treated as vibrations and tunneling evaluated with the Eckart model.

3. Results and Discussion

3.1 Rate coefficients

Table 1S summarizes conditions of 10 determinations of k_1 at room temperature. The standard deviation σ is the uncertainty of plots of the exponential decay constant k_{ps1} vs 5 values of [N_2H_4], from zero to the tabulated maximum value. Within the scatter of the data, there is no dependence of the rate constant on the experimental parameters τres, F, E and total pressure. The UV pulse energy F and [NH_3] control [NH_2]$_0$ and were varied to check whether the observed kinetics were affected by secondary chemistry. The lack of dependence indicates that reaction 1 was successfully isolated. The weighted mean value of k_1 is 5.4 × 10^{-14} cm^3 molecule^{-1} s^{-1} at 296 K. 2σ combined in quadrature with an allowance of up to 5% for systematic errors in T, P and hence concentrations leads to a 95% confidence interval of ±0.4 × 10^{-14} cm^3 molecule^{-1} s^{-1}.

We note that this result is almost an order of magnitude below the value derived by Gehring et al. [5] from flow reactor results for N_2H_4/H_2/H mixtures. They based their determination on measured concentrations of N_2H_4, N_2H_3, NH_3, NH_2, and H_2 as a function of reaction time. However, due to the differences in their values obtained for H + N_2H_4 compared to other measurements (see Fig. 2), Vaghjiani [8] proposed that Gehring et al. may have had errors in the absolute reagent calibration in their work. Furthermore, our modeling of their results (see the beginning of Section 3.2 for the description of the mechanism) indicates that the sensitivity towards NH_2 + N_2H_4 is limited and that formation of NH_3, used as a marker for R1, occurs via H + NH_2 recombination to a significant extent. For these reasons, their proposed rate constant is associated with a significant uncertainty.

At higher temperatures dependence on residence time was observed, perhaps reflecting surface loss of hydrazine, and the results were highly scattered. Accordingly, we rely on theoretical methods to extrapolate k_1 to higher temperatures.

Table S2 provides the Cartesian coordinates of transition states (TSs) for reaction 1, and the three TS structures are drawn in Fig. 3. Their relative energies with CCSD(T)-F12b theory are provided in Table S3, with W1U values for comparison, and the correction ΔQ for inclusion of quadruple excitations with perturbation theory for the electron correlation.

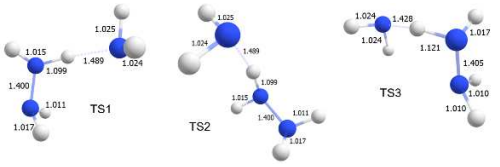

Fig. 3. Structures of three transition states for NH_2 + N_2H_4 with bond lengths in 10^{-10} m, computed with M06-2X/6-311+G(2df,2p) theory.

Relative enthalpies for R1 are shown in Fig. 4.

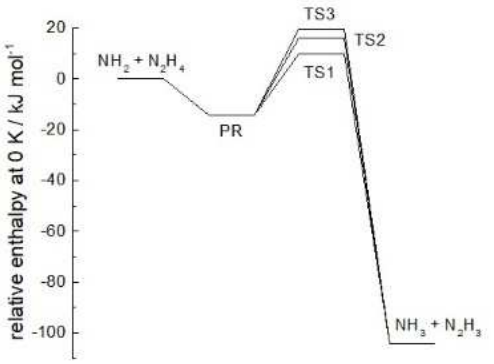

Fig. 4. CCSD(T)-F12+ΔQ+zpe enthalpy diagram for the NH_2 + N_2H_4 reaction.

Hydrogen bonding between the reactants is likely, and the structure of an example pre-reactive complex is provided in Fig. 1S. The binding energy of 14.2 kJ mol^{-1} is too small for this complex to be stable at room temperature or above. From a microscopic point of view, there will be little population of its energy levels below the energy of the reactants, which would require rapid collisional stabilization of the levels initially populated at or slightly above the reactants' energy before dissociation back to the reactants or further reaction, and even if a very high pressure of bath gas was employed, the micro-canonical equilibrium with the reactants is unfavorable. Thus the weak pre-reactive complex does not affect the kinetics (except at lower temperatures than relevant here). The enthalpies relative to reactants at 0 K, including zero-point energy, at the CCSD(T)-F12+ΔQ for TS1, TS2 and

TS3 are computed to be 9.8, 16.1 and 19.7 kJ mol^{-1}, respectively. As a check on the reliability of these quantities, we note that at this level the overall reaction enthalpy Δ_rH_0 = -104.4 kJ mol^{-1} is the same as the ATcT recommended value of -104.4 ± 0.8 kJ mol^{-1} [27]. Accuracy may be assisted by the fact that R1 is isodesmic.

The multistructural TST analysis yields $k_1 = 6.3 \times 10^{-23}$ $T^{3.44}$ exp(-49 K/T) cm^3 molecule^{-1} s^{-1}, the black dashed curve on Fig. 1. This is in fair agreement with our room temperature measurement, to within about a factor of 3. The solid black curve shows the effect of lowering the barrier by 2.8 kJ mol^{-1}. This empirical correction may address factors such as neglect of electron correlation beyond perturbative quadruple excitations and the finite basis set, or can simply be viewed as a fix to ensure a match with experiment. Our final recommendation for extrapolation of the measured room temperature value to higher temperatures is $k_1 = 6.3 \times 10^{-23}$ $T^{3.44}$ exp(+289 K/T) cm^3 molecule^{-1} s^{-1}.

We note this result agrees to just within the quoted uncertainty [4] with the result from Meyer et al. It is significantly above the prior theoretical analysis of Li and Zhang [3]. Our computational approach yields similar barriers: for TS1 we obtained a classical barrier (without zero-point energy) of 11.2 kJ mol^{-1} (before the empirical correction), whereas the earlier MC-QCISD result [28] was 10.6 kJ mol^{-1}, so the variance presumably arises from the multistructural treatment of coupled torsions. There is close accord with the expression of Dean and Bozzelli, who made empirical estimates of the A and m parameters in a modified Arrhenius expression A T^m exp(-E/RT) and based E on an Evans-Polanyi correlation with reaction enthalpy [7]. The agreement with their DHT method suggests our recommendation for R1 is in accord with analogous hydrogen transfer reactions.

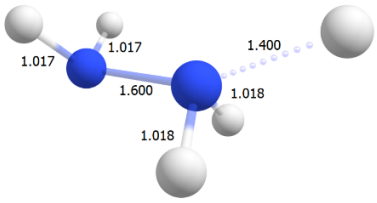

Fig. 5. Structure of the transition state for H + N_2H_4 → NH_3 + NH_2 with bond lengths in 10^{-10} m, computed with M06-2X/6-311+G(2df,2p) theory.

For reaction 2b, the TS structure is shown in Fig. 5. The computed reaction enthalpy with CCSD(T)-F12b/pVQZ-F12 theory at 0 K is Δ_rH_0 = -177.7 kJ mol^{-1}, in good agreement with the recommended value of -177.4 ± 0.4 kJ mol^{-1} [27]. The forward barrier (including zero-point energy) is computed to be 45.7 kJ mol^{-1} at 0 K. Canonical TST yields k_{2b} = 5.0×10^{-19} $T^{2.07}$ exp(-4032 K/T) cm^3 molecule^{-1} s^{-1}. This result confirms the previous calculation by Hwang and Mebel [12], as seen in Fig. 2, but there are large differences from the assessment by Konnov and De Ruyck [6]. They used the ratio k_{2c}/k_2 from chemiluminescence measurements [11] as equivalent to k_{2b}/k_2. These experiments may be hard to interpret, since the excited potential energy surface leading to excited NH_2^* need not have the same barrier as the ground-state surface, and because NH_2^* might originate from processes other than R2c. With a large excess of H over N_2H_4, we expect extensive transformation to NH_2 via fast reaction of the major initial abstraction product N_2H_3 with H to make 2 NH_2, and speculate that energy can in some collisions be transferred from recombining H + NH_2 or NH_2 + NH_2 to another NH_2. Another potential source of NH_2^* is NH + H addition, by analogy with O + H addition that leads to OH^* emission in flames.

3.2 Implications for hydrazine reactivity

In this section, we discuss the impact of the NH_2 + N_2H_4 reaction on hydrazine pyrolysis, and briefly evaluate the capability of the present mechanism to describe this chemistry. Much of the work on N_2H_4 pyrolysis was reviewed by Konnov and De Ruyck [6], who also established a detailed kinetic model for its decomposition. Since their work, a number of theoretical studies relevant to the hydrazine decomposition chemistry have been published. Klippenstein et al. [29] calculated rate constants for reactions on the N_2H_4 potential energy surface, including recombination of NH_2 radicals to form N_2H_4 (R3), while Grinberg Dana et al. [30], Diévart and Catoire [31], and Marshall et al. [32] investigated reactions of N_2H_3 and HNNH. The chemical kinetic model used here, including rate coefficients and thermodynamic data (Tables S4 and S5), is based mainly on the review of nitrogen chemistry by Glarborg et al. [33], with updates from recent work on amine pyrolysis [30-32] and oxidation [34, 35].

We have compared the hydrazine half-lives reported from pyrolysis in reflected shock tube experiments by Michel and Wagner [36] with modeling predictions. These experiments were conducted at medium temperatures with N_2H_4 mole fractions of around 0.3%. Under these conditions secondary reactions play a role in addition to thermal dissociation of hydrazine.

Figure 6 shows the impact of modeling assumptions on the prediction of hydrazine decomposition during pyrolysis at 1100 K and 7.6 atm. Predictions with a 1-step model (short-dashed line) including only thermal dissociation of hydrazine [29] indicate a decomposition rate well below that observed experimentally by Michel and Wagner. If N_2H_4 + NH_2 = N_2H_3 + NH_3 (R1) is added (the 2-step model; long-dashed line), the consumption rate of hydrazine is increased by a factor of three, providing a much better agreement

with experiment. In the 2-step model, the amidogen radical reacts selectively with hydrazine and R3 is the rate limiting step.

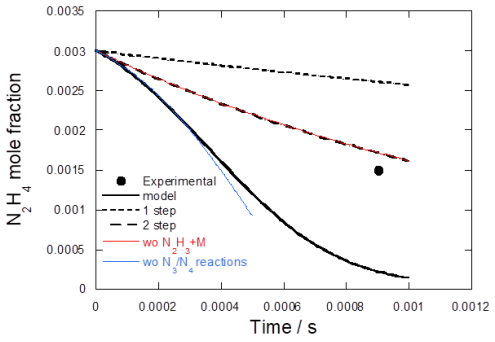

Fig. 6. Impact of modeling assumptions on the prediction of hydrazine decomposition at 1100 K and 7.6 atm. The experimental data point was obtained by Michel and Wagner [36] behind reflected shock waves. In addition to predictions with the full model, calculations are shown for a 1-step model (N_2H_4 (+Ar) → products), a 2-step model (N_2H_4 (+Ar) = NH_2 + NH_2 (+Ar), N_2H_4 + NH_2 = N_2H_3 + NH_3), and the full mechanism with either thermal dissociation of N_2H_3 or reactions on the N_3H_5 and N_4H_6 PES [37] omitted.

The full model overpredicts the hydrazine decomposition rate (the black solid line in Fig. 6). A sensitivity analysis shows that dissociation of N_2H_4 to NH_2 + NH_2 (R3b) is the major rate controlling step, followed by NH_2 + N_2H_4 (R1) and N_2H_3 dissociation. The rate constant for thermal dissociation of N_2H_4 (R3) is now well established, with a recent analysis by Cobos et al. [38] essentially supporting the value calculated by Klippenstein et al. [29]. Even though R3 has the largest sensitivity coefficient in predicting the concentration profile of N_2H_4, secondary reactions play a significant role.

The difference in predictions between the full model and the 2-step model is caused by the fate of the N_2H_3 radical, which to a large extent controls the production of chain carriers in the system. If dissociation of N_2H_3 to form HNNH + H is removed from the mechanism, predictions become identical to those of the 2-step model. The hydrogen atom formed in the dissociation may abstract H from hydrazine to form N_2H_3 + H_2 or boost the radical pool in a reaction with N_2H_3 to form 2 NH_2. The N_2H_3 + H → NH_2 + NH_2 proceeds without a barrier and is expected to be very fast [32], while N_2H_3 + H → HNNH + H_2 is only a minor channel. Formation of NH_3 + NH_2 from N_2H_4 + H (R2b) is too slow to compete with H-abstraction (R2a) and does not contribute to NH_3 production at the temperatures of interest.

The predicted consumption rate of hydrazine is thus to a large extent determined by the competition between propagating and chain terminating steps of N_2H_3. The N_2H_3 subset of the mechanism involves major uncertainties. The thermal dissociation of N_2H_3 has not been determined experimentally; the rate constant adopted in the model was calculated by Diévart and Catoire [31]. The dissociation competes with chain terminating reactions involving N_2H_3, such as N_2H_3 + NH_2 → (diazene isomer) + NH_3, N_2H_3 + NH_2 (+M) → N_3H_5 (+M), N_2H_3 + N_2H_3 → (diazene isomer) + N_2H_4, and N_2H_3 + N_2H_3 (+M) → N_4H_6 (+M). Experimental data for these steps are lacking, but the reactions have been studied theoretically. Grinberg Dana et al. [30] calculated rate constants for reactions on the N_3H_5 potential energy surface (PES), including N_2H_3 + NH_2. At 1100-1400 K and 10 atm, the dominating reaction channels for N_2H_3 + NH_2 were found to be H-abstraction to form H_2NN + N_2H_4 and recombination to N_3H_5, respectively, with a combined rate constant of about 5×10^{12} cm^3 mol^{-1} s^{-1}. Diévart and Catoire [31] only reported data for the H-abstraction channels to form a diazene isomer and N_2H_4, with a total rate constant in the range 5×10^{10} - 1.2×10^{11} cm^3 mol^{-1} s^{-1}; well below the values calculated by Grinberg Dana et al. For N_2H_3 + N_2H_3, an early experimental study by Stief [37] indicated that disproportionation dominates over combination at low temperature, but the study did not involve any direct measurements. According to Grinberg Dana et al. [30], recombination to N_4H_6 dominates at 1100 K and 10 atm with a rate constant of almost 1×10^{11} cm^3 mol^{-1} s^{-1}. Disproportionation is predicted to be quite slow, while a channel to N_3H_4 + NH_2 becomes dominant at higher temperatures.

Compared to our earlier model [31], we have updated the N_2-amine subset with the reactions and rate constants calculated by Grinberg Dana et al. [30]. This change improves slightly predictions, as shown in Fig. 6, due to the faster rate constant for N_2H_3 + NH_2 and inclusion of N_2H_3 + N_2H_3, but the calculated hydrazine decomposition is still too fast. To obtain a better agreement with experiment, a lower rate constant for dissociation of N_2H_3 or a higher rate constant for either N_2H_3 + NH_2 (2×10^{13} cm^3 mol^{-1} s^{-1}) or N_2H_3 + N_2H_3 (1×10^{12} cm^3 mol^{-1} s^{-1}) going to stable products would be required. Such changes are presumably within the uncertainty of the current values.

Conclusions

A combined experimental and computational approach is applied to the kinetics of NH_2 + N_2H_4, where there have been significant differences between earlier estimates. Direct measurements at high temperatures would be valuable. Modeling confirms that an accurate rate coefficient is important for reliable predictions of hydrazine decomposition. However, calculations are also sensitive to several reactions of N_2H_3 and HNNH, and more work is needed on the hydrazine subset to

ensure satisfactory predictions of high temperature amine chemistry.

Acknowledgements

PM thanks the U.S. Department of Energy, Office of Basic Energy Sciences, Division of Chemical Sciences, Geosciences and Biosciences/Gas Phase Chemical Physics under Contract No. DESC0020952. Computational facilities were provided by the National Science Foundation, Grant CHE-1531468. PG and HH acknowledge funding from Innovation Fund Denmark for the AEngine Grand Solutions project.

References

[1] H. Kobayashi, A. Hayakawa, K.D.K.A. Somarathne, E.C. Okafor, Science and technology of ammonia combustion, *Proc. Combust. Inst.* 37 (2019) 109-133.

[2] A. Valera-Medina, F. Amer-Hatem, A.K. Azad, I. Dedoussi, M. De Joannon, R.X. Fernandes, P. Glarborg, H. Hashemi, X. He, S. Mashurk, J. McGowan, C. Mounaim-Rouselle, A. Ortiz-Prado, J.A. Ortiz-Valera, I. Rossetti, B. Shu, M. Yehia, H. Xiao, M. Costa, A review on ammonia as a potential fuel: from synthesis to economics, *Energy Fuels* 35 (2021) 6964-7029.

[3] Q.S. Li, X. Zhang, Direct dynamics study on the hydrogen abstraction reactions N_2H_4+R → N_2H_3+RH (R=NH_2, CH_3), *J. Chem. Phys.* 125 (2006) 064304.

[4] E. Meyer, H.A. Olschewski, J. Troe, H.G. Wagner, Investigation of N_2H_4 and H_2O_2 decomposition in low and high pressure shock waves, *Symp. (Int.) Combust.* 12 (1969) 345-355.

[5] M. Gehring, K. Hoyermann, H.G. Wagner, J. Wolfrum, Die Reaktion von Atomarem Wasserstoff mit Hydrazin, *Ber. Bunsenges. Phys. Chem.* 75 (1971) 1287-1294.

[6] A.A. Konnov, J.D. Ruyck, Kinetic modeling of the decomposition and flames of hydrazine, *Combust. Flame* 124 (2001) 106-126.

[7] A.M. Dean, J.W. Bozzelli, Combustion Chemistry of Nitrogen, in: W.C. Gardiner, Jr. (Ed.), Gas-Phase Combustion Chemistry, Springer-Verlag, New York, 2000, pp. Ch. 2.

[8] G.L. Vaghjiani, Laser photolysis studies of hydrazine vapor: 193 and 222-nm H-atom primary quantum yields at 296 K, and the kinetics of H + N_2H_4 reaction over the temperature range 222-657 K, *Int. J. Chem. Kinet.* 27 (1995) 777-790.

[9] Q.S. Li, X. Zhang, S.W. Zhang, Direct Dynamics Study on the Hydrogen Abstraction Reaction N_2H_4 + H → N_2H_3 + H_2, *J. Phys. Chem. A* 107 (2003) 6055-6061.

[10] N. Kanno, T. Kito, Theoretical study on the hydrogen abstraction reactions from hydrazine derivatives by H atom, *Int. J. Chem. Kinet.* 52 (2020) 548-555.

[11] P.K. Ghosh, E.J. Bair, Reactions of Nitrogen-Hydrogen Radicals. II. Decomposition of Hydrazine by Hydrogen Atoms, *J. Chem. Phys.* 45 (1966) 4738-4741.

[12] D.-Y. Hwang, A.M. Mebel, Reaction Mechanism of N_2/H_2 Conversion to NH_3: A Theoretical Study, *J. Phys. Chem. A* 107 (2003) 2865-2874.

[13] S.A. Alturaifi, O. Mathieu, E.L. Petersen, An experimental and modeling study of ammonia pyrolysis, *Combust. Flame* 235 (2021) 111694.

[14] Y. Gao, P. Marshall, Kinetic Studies of the Reaction NH_2 + H_2S, *Chem. Phys. Lett.* 594 (2014) 30-33.

[15] Y. Gao, P. Glarborg, P. Marshall, The Reaction Kinetics of Amino Radicals with Sulfur Dioxide, *Z. Phys. Chem.* 229 (2015) 1649-1661.

[16] M.J. Frisch, G.W. Trucks, H.B. Schlegel, G.E. Scuseria, M.A. Robb, J.R. Cheeseman, G. Scalmani, V. Barone, G.A. Petersson, H. Nakatsuji, X. Li, M. Caricato, A.V. Marenich, J. Bloino, B.G. Janesko, R. Gomperts, B. Mennucci, H.P. Hratchian, J.V. Ortiz, A.F. Izmaylov, J.L. Sonnenberg, Williams, F. Ding, F. Lipparini, F. Egidi, J. Goings, B. Peng, A. Petrone, T. Henderson, D. Ranasinghe, V.G. Zakrzewski, J. Gao, N. Rega, G. Zheng, W. Liang, M. Hada, M. Ehara, K. Toyota, R. Fukuda, J. Hasegawa, M. Ishida, T. Nakajima, Y. Honda, O. Kitao, H. Nakai, T. Vreven, K. Throssell, J.A. Montgomery Jr., J.E. Peralta, F. Ogliaro, M.J. Bearpark, J.J. Heyd, E.N. Brothers, K.N. Kudin, V.N. Staroverov, T.A. Keith, R. Kobayashi, J. Normand, K. Raghavachari, A.P. Rendell, J.C. Burant, S.S. Iyengar, J. Tomasi, M. Cossi, J.M. Millam, M. Klene, C. Adamo, R. Cammi, J.W. Ochterski, R.L. Martin, K. Morokuma, O. Farkas, J.B. Foresman, D.J. Fox, Gaussian 16 Rev. A.03, Wallingford, CT, (2016).

[17] I.M. Alecu, J. Zheng, Y. Zhao, D.G. Truhlar, Computational Thermochemistry: Scale Factor Databases and Scale Factors for Vibrational Frequencies Obtained from Electronic Model Chemistries., *J. Chem. Theory Comput.* 6 (2010) 2872-2887.

[18] H.J. Werner, P.J. Knowles, R. Lindh, F.R. Manby, M. Schutz, P. Celani, T. Korona, A. Mitrushenkov, G. Rauhut, T.B. Adler, R.D. Amos, A. Bernhardsson, A. Berning, D.L. Cooper, M.J.O. Deegan, A.J. Dobbyn, F. Eckert, E. Goll, C. Hampel, G. Hetzer, T. Hrenar, G. Knizia, C. Koppl, Y. Liu, A.W. Lloyd, R.A. Mata, A.J. May, S.J. McNicholas, W. Meyer, M.E. Mura, A. Nicklass, P. Palmieri, K. Pfluger, R. Pitzer, M. Reiher, U. Schumann, H. Stoll, A.J. Stone, R. Tarroni, T. Thorsteinsson, M. Wang, A. Wolf, *MOLPRO*, version 2010.1, (2010).

[19] J.M.L. Martin, G. de Oliveira, Towards Standard Methods for Benchmark Quality *Ab Initio* Thermochemistry - W1 and W2 Theory., *J. Chem. Phys.* 111 (1999) 1843-1856.

[20] T. Yu, J. Zheng, D.G. Truhlar, Multi-Structural Variational Transition State Theory: Kinetics of the 1,4-Hydrogen Shift Isomerization of the Pentyl Radical with Torsional Anharmonicity, *Chem. Sci.* 2 (2011) 2199-2213.

[21] Y.-P. Liu, D.-H. Lu, A. Gonzàlez-Lafont, D.G. Truhlar, B.C. Garrett, Direct dynamics calculation of the kinetic isotope effect for an organic hydrogen-transfer reaction, including corner-cutting tunneling in 21 dimensions, *J. Am. Chem. Soc.* 115 (1993) 7806-7817.

[22] J. Zheng, S. Zhang, B.J. Lynch, J.C. Corchado, Y.-Y. Chuang, P.L. Fast, W.-P. Hu, Y.-P. Liu, G.C. Lynch, K.A. Nguyen, C.F. Jackels, A.F. Ramos, B.A. Ellingson, V.S. Melissas, J. Villà, I. Rossi, E.L. Coitiño, J. Pu, T.V. Albu, R. Steckler, B.C. Garrett, A.D. Isaacson, D.G. Truhlar, POLYRATE: Computer Program for the Calculation of Chemical Rates for Polyatomics, version 2010-A; University of Minnesota: Minneapolis, MN, (2010).

[23] J. Zheng, S.L. Mielke, K.L. Clarkson, D.G. Truhlar, MSTor: A program for calculating partition functions, free energies, enthalpies, and entropies of complex molecules

including torsional anharmonicity, version 2011-3, University of Minnesota, Minneapolis, MN, (2012).
[24] I.M. Alecu, Y. Gao, P. Marshall, Experimental and Computational Studies of the Kinetics of the Reaction of Hydrogen Peroxide with the Amidogen Radical, *J. Chem. Phys.* in press.
[25] J.C. Rienstra-Kiracofe, W.D. Allen, H.F. Schaefer III, The $C_2H_5 + O_2$ Reaction Mechanism: High-Level ab Initio Characterizations, *J. Phys. Chem. A* 104 (2000) 9823-9840.
[26] J.R. Barker, T.L. Nguyen, J. Stanton, C. Aieta, M. Ceotto, F. Gabas, T.J.D. Kumar, C.G.L. Li, L.L. Lohr, A. Maranzana, N.F. Ortiz, J.M. Preses, J.M. Simmie, J.A. Sonk, P.J. Stimac, MultiWell-2021, University of Michigan, Ann Arbor, MI, 2021, http://aoss-research.engin.umich.edu/multiwell/.
[27] B. Ruscic, D.H. Bross, Active Thermochemical Tables, version 1.122p, http://atct.anl.gov (accessed April, 2021). Argonne National Laboratory, Lemont, IL.
[28] P.L. Fast, D.G. Truhlar, MC-QCISD: multi-coefficient correlation method based on quadratic configuration interaction with single and double excitations, *J. Phys. Chem. A* 104 (2000) 6111-6116.
[29] S.J. Klippenstein, L.B. Harding, B. Ruscic, R. Sivaramakrishnan, N.K. Srinivasan, M.-C. Su, J.V. Michael, Thermal decomposition of NH_2OH and subsequent reactions: Ab initio transition state theory and reflected shock tube experiments, *J. Phys. Chem. A* 113 (2009) 10241-10259.
[30] A.G. Dana, K.B.M. III, A.W. Jasper, W.H. Green, Large Intermediates in Hydrazine Decomposition: A Theoretical Study of the N_3H_5 and N_4H_6 Potential Energy Surfaces, *J. Phys. Chem. A* 123 (2019) 4679-4692.
[31] P. Diévart, L. Catoire, Contributions of Experimental Data Obtained in Concentrated Mixtures to Kinetic Studies: Application to Monomethylhydrazine Pyrolysis, *J. Phys. Chem. A* 124 (2020) 6214−6236.
[32] P. Marshall, G. Rawling, P. Glarborg, New reactions of diazene and related species for modeling combustion of amine fuels, *Mol. Phys.* 119 (2021) e1979674.
[33] P. Glarborg, J.A. Miller, B. Ruscic, S.J. Klippenstein, Modeling Nitrogen Chemistry in Combustion, *Prog. Energy Combust. Sci.* 67 (2018) 31-68.
[34] A. Stagni, C. Cavallotti, S. Arunthanayothin, Y. Song, O. Herbinet, F. Battin-Leclerc, T. Faravelli, An experimental, theoretical and kinetic-modeling study of the gas-phase oxidation of ammonia, *React. Chem. Eng.* 5 (2020) 696−711.
[35] S.J. Klippenstein, P. Glarborg, Theoretical Kinetics Predictions for $NH_2 + HO_2$, *Combust. Flame* 236 (2022) 111787.
[36] K.W. Michel, H.G. Wagner, Untersuchung des thermischen zerfalls und der oxydation von hydrazin mit stoßwellen, *Z. Phys. Chem.* 35 (1962) 392-395.
[37] L.J. Stief, Ratio of disproportionation to combination of N_2H_3 radicals, *J. Chem. Phys.* 52 (1970) 4841-4845.
[38] C.J. Cobos, P. Glarborg, P. Marshall, J. Troe, Re-evaluation of rate constants for the reaction N_2H_4 (+ M) ⇄ $NH_2 + NH_2$ (+ M), *submitted* (2022).